Inelastic and anomalous elastic scattering of 88.03-keV γ rays

P. P. Kane,* G. Basavaraju, Saharsha M. Lad, and K. M. Varier†
Department of Physics, Indian Institute of Technology, Powai, Bombay 400 076, India

Lynn Kissel‡ and R. H. Pratt
Department of Physics and Astronomy, University of Pittsburgh, Pittsburgh, Pennsylvania 15260
(Received 14 May 1987)

Cross sections for the elastic scattering of 88.03-keV γ rays through 125° by aluminum, gold, lead, and bismuth have been measured with a semiconductor detector. Simultaneously, information has been obtained regarding resonance Raman scattering and Compton scattering in the case of bismuth, and K-shell photoeffect cross sections in the case of gold and lead. Values accurate to about 8% were determined with the help of a normalization technique relying on a comparison with the Compton scattering counts from the low-atomic-number aluminum target. The elastic scattering cross section of aluminum at the chosen photon energy, which is far above the aluminum K-shell threshold, is in reasonable accord with form-factor and S-matrix calculations based on the independent-particle approximation. For gold, 7.3 keV above its threshold, the experiment agrees with the S-matrix prediction. However, for lead some 25 eV above threshold, the experimental value is about 40% larger than predicted, while for bismuth (2.5 keV *below* threshold), experiment lies 70% above theory. The measured K-shell photoeffect cross section of lead is within 10% of the prediction based on the independent-particle approximation.

I. INTRODUCTION

A cadmium-109 source is a popular choice in the application of the x-ray fluorescence (XRF) technique to the determination of concentrations of trace elements in different types of samples. While using the XRF technique in conjunction with an annular source and a Si(Li) detector, we thought it worthwhile to study selected photon-atom cross sections with the same experimental arrangement. The low efficiency of detection of a Si(Li) counter has generally discouraged the use of this counter for γ-ray energies above about 40 keV. However, as we shall show, the cylindrical symmetry of the adopted arrangement enables fairly precise measurements to be made even with such a counter and sources of only a few millicurie strength. Note also that, unlike in the case of germanium counters, escape peak corrections are small in the case of Si(Li) counters.

The 88.03-keV γ energy from a cadmium-109 source is only about 25 eV higher than the K-shell binding energy of lead (88.006 keV) and about 2.5 keV lower than the K-shell binding energy of bismuth (90.527 keV). To our knowledge, anomalous scattering amplitudes have not so far been studied in the close vicinity of K-shell binding energies of such high-Z atoms. Previous studies of anomalous scattering have been summarized in recent reviews.[1,2] Further, accurate theoretical values of elastic scattering cross sections of lead for 88-keV γ rays recently became available.[3] The calculations indicated that near $x=6.3$ the real parts of the scattering amplitudes make a very small contribution to the lead elastic scattering cross section. Here, $x=\sin(\theta/2)/\lambda(\text{Å})$, θ is the angle of scattering and λ (Å) is the wavelength of the γ radiation in angstroms. Accordingly, measurements were made at a mean scattering angle of 125° in an effort to understand the salient features of the anomalous elastic scattering amplitudes. The imaginary amplitudes due to the bismuth K-shell are, of course, zero at 88.03 keV. Since the photon energy is as much as 7.3 keV larger than the gold K-shell binding energy, the anomalous scattering contributions are less important in the case of gold than in the case of lead and bismuth. Since all electrons in a low-Z element such as aluminum are weakly bound, the scattering cross sections for this case calculated in the form-factor approximation with minor corrections[3] can be used to check the accuracy of the experimental values. New S-matrix calculations have also been performed in support of this experiment.

Since the chosen photon energy is lower than the bismuth K-shell binding energy, there was clearly a possibility of a simultaneous study of the recently discovered process of x-ray resonance Raman scattering (RRS) corresponding to virtual K-L_2, K-L_3, K-$M_{2,3}$ transitions. After our work was completed, we saw a published report[4] concerning this aspect. That report is, however, not concerned with the measurement of elastic scattering cross sections. As a by-product of our main investigation, we have observed K-L_2 and K-$M_{2,3}$ RRS in bismuth but are unable to report accurate values of RRS cross sections due to complications arising from a possible higher-energy weak contamination present in the source (see Sec. II for more details regarding the contamination).

The photoelectrons ejected from the lead K shell by 88.03-keV γ rays have a maximum kinetic energy of only about 25 eV. On the other hand, the K-shell hole state in a high-Z element such as lead has a width of about 66 eV (Ref. 5) and so a mean life of about 10^{-17} s.

The time required for the 25-eV electron to emerge out of the lead atom will be a significant fraction (~ 0.3) of the decay time of the hole state. Thus the usually assumed separability of the two processes of vacancy creation and subsequent decay is not sharp in the lead case under discussion. Note that the width of a K-shell hole state decreases rapidly with decreasing Z and is, for example, only about 1.2 eV in the case of nickel. Therefore, even though resonance Raman scattering experiments have been performed with finely tuned synchrotron radiation and a nickel target,[6] situations involving a photoelectron energy considerably smaller than the hole state width have not been adequately studied as yet. We may also ask whether in such circumstances, and so close to threshold, an independent-particle description of elastic scattering remains appropriate.

As a by-product, we also determined the incoherent scattering function of bismuth at a mean x value of 6.3, and the K-shell photoeffect cross sections in the case of gold and lead. Since the intense $K\alpha$ x-ray peaks overlap to a significant extent, the broad Compton peak centered at about 69.3 keV; the overlap being less in the case of lead than that in the case of gold, the incoherent scattering functions of gold and lead could not be determined in this experiment.

The details of experimental procedures are described in Sec. II. The results are presented and discussed in Sec. III in the light of available theoretical calculations. In the same section, suggestions are given for more detailed experimental and theoretical studies.

II. EXPERIMENTAL PROCEDURES

The experimental arrangement is shown in Fig. 1. The annular cadmium-109 source supplied by Amersham had a strength of about 3 mCi. It was housed in a stainless-steel holder containing heavy tungsten alloy shielding and capped with a berryllium window. The targets were fixed to very thin sticking tapes which were mounted on thin aluminum rings. The source holder and the target mounting ring were held fixed in a specially made cylindrical aluminum shell (not shown) which fitted snugly onto the horizontal detector arm. The reproducibility of the short source-target and target-detector distances was checked by making measurements of counting rates with the same target after several operations involving the placement and removal of the target mounting ring. A 1-mm-thick cylindrical sleeve of tantalum was found to be useful in reducing higher-energy radiation background not completely absorbed by the thin sides of the stainless-steel holder. Aluminum, gold, and lead foils of better than 99% purity were used as targets. Relatively thin targets with effective transmission factors in the neighborhood of 0.8 were used. The thicknesses of the aluminum, gold, and lead targets were 212, 27.4, and 19.2 mg/cm^2, respectively. Analytical reagent grade bismuth in the form of $Bi(NO_3)_3 \cdot 5H_2O$ powder was crushed in a mortar and formed under pressure into a pellet of 139 mg/cm^2 thickness. The Si(Li) detector of 0.5 cm thickness and 1.6 cm diameter was supplied by EG&G ORTEC. The full width at half maximum was about 630 eV for 88-keV γ rays. The large flux of scattered silver K x rays was attenuated with the help of a graded copper-aluminum absorber in front of the detector with the aluminum surface facing the detector. The thicknesses of copper and aluminum were 0.010 and 0.100 cm, respectively. The absorber was helpful in reducing the total counting rate to less than 70 per second. Thus effects due to pileup were negligible. The transmission of the absorber for 88-keV γ rays was as high as 0.908.

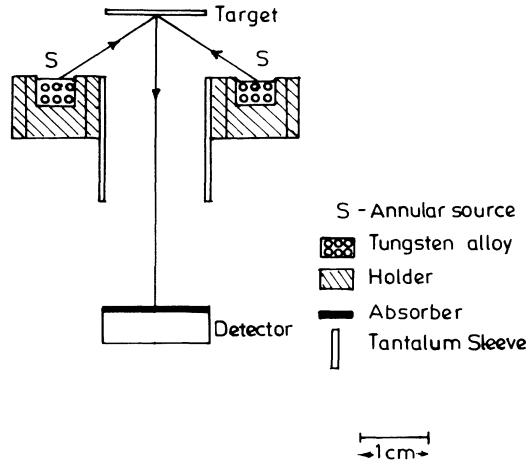

FIG. 1. Experimental arrangement.

The net count rate due to a given target was determined from the difference between the target-in and target-out rates. Any cross section of interest was obtained by comparing the corresponding net count rate n with the net count rate n^C_{Al} determined from the Compton peak with an aluminum target of the same area and a known number of atoms. The method described previously[7] relies on the fact that the Compton scattering cross section of a low-Z element like aluminum is given accurately by the product of the Klein-Nishina expression and the incoherent scattering function $S(x,Z)$. Nonrelativistic values of $S(x,z)$ are available in tabular form.[8] With this method, the source intensity and solid angle factors are eliminated, and a knowledge of the absolute value of the detection efficiency is not required. Let us suppose that the elastic scattering cross section $d\sigma_{el}/d\Omega$ of a target atom is to be measured. Then

$$\frac{n_{el}}{n^C_{Al}} = \frac{N_{sc}}{N_{Al}} \frac{\dfrac{d\sigma_{el}}{d\Omega}}{\left[\dfrac{d\sigma^C}{d\Omega}\right]_{Al}} \frac{T^{88}_{sc}}{T^C_{Al}} \frac{T^{88}_A}{T^C_A} \frac{\eta^{88}}{\eta^C} , \tag{1}$$

where N_{sc} is the number of target atoms and is proportional to $\rho t/A'$, ρt is the mass of the target per unit area, A' is the atomic weight of the scatterer, N_{Al} is the number of atoms in the aluminum target, $(d\sigma^C/d\Omega)_{Al}$ is the Compton scattering cross section of aluminum, T^{88}_{sc} and T^C_{Al} are, respectively, the average transmission factors of the scatterer at 88 keV and of aluminum for Compton-scattered photons, T^{88}_A and T^C_A are the

transmission factors of the previously mentioned absorber at 88 keV and for Compton-scattered photons, and η^{88} and η^{C} are the photopeak efficiencies of the detector at 88 keV and at the Compton energy. Measurements were made in each case with two additional targets of thickness larger than the ones mentioned earlier in order to verify the absence of any significant secondary effects such as bremsstrahlung generated in the target. Since thin targets were used for determination of cross sections, the errors in the ratios of transmission factors are only of the order of 1.5%.

It should be noted that the ratio η^{88}/η^{C} of photopeak efficiencies is required only over an energy range from about 65 to 88 keV. It is known[9] that errors in absolute efficiencies can be large and are not easily determined. It is for this reason that a measurement technique relying on a ratio of efficiencies is desirable. Calculated values concerning variation of detector efficiency with photon energy were supplied by ORTEC in a graphical form. These data were checked by us in the following way. With targets of gold and lead, prominent $K\alpha_2$, $K\alpha_1$, $K\beta_1'$, and $K\beta_2'$ x-ray peaks are observed at energies varying between 66.99 and 87.36 keV. Suppose that we compare measured intensities n_i and n_j of the ith and the jth K x-ray peaks of a given target. Then

$$\frac{n_i}{n_j}=\frac{\alpha_i}{\alpha_j}\frac{T^i_{\rm sc}}{T^j_{\rm sc}}\frac{T^i_A}{T^j_A}\frac{\eta^i}{\eta^j}\ , \tag{2}$$

where α_i and α_j are the branching ratios for the K x-ray transitions labeled i and j, the transmission factors are evaluated for energies of peaks i and j, and η^i/η^j is the ratio of detector efficiencies for energies of peaks i and j.

The values of α_i and α_j were taken from the work of Scofield.[10] Recent experimental work[11] concerning the above-mentioned branching ratios has clarified the origin of inaccuracies in earlier data and has also confirmed Scofield's calculated values. The intensities of the peaks were determined by the method of least squares. A Gaussian and a polynomial continuum were adequate for the representation of most peaks except the lead $K\beta_2'$ x rays and the bismuth $K\beta_1'$ x rays. For example, in the lead case, four Gaussians representing the lead $K\beta_2'$ x rays were necessary. The value of χ^2 in each case was approximately unity. The error in the ratio n_i/n_j of intensities is less than 3%. The error in the calculated ratio α_i/α_j is expected to vary between about 1–3 %. The error in the measured value of η^i/η^j is thus about ±4% in most cases. The experimental value of η at gold $K\alpha_1$ energy of 68.80 keV was normalized to that shown by the manufacturer. The relative error in reading the value of the efficiency from the curve supplied by the manufacturer is variable and is as high as 4% near the high-energy end of 90 keV. The data are presented in Fig. 2. The agreement between the solid curve based on manufacturer's data and our measured values is quite good. In reporting the values of cross sections a value of ±5% has been adopted as the error in the efficiency ratio in Eq. (1).

Net counts obtained with an aluminum target in the neighborhood of the Compton peak in a counting time of 23 h are shown in Fig. 3. From the width of the broad Compton peak, the angular acceptance in the experiment can be directly estimated to be ±12°. The use of the tantalum sleeve is responsible for the tantalum K x-ray peaks noticeable in the figure. Similar data in the neighborhood of the Compton peak obtained with the bismuth target are not shown. Data obtained near 88 keV with gold and bismuth targets are presented in Fig. 4. The gold data reveal a clean elastic scattering peak

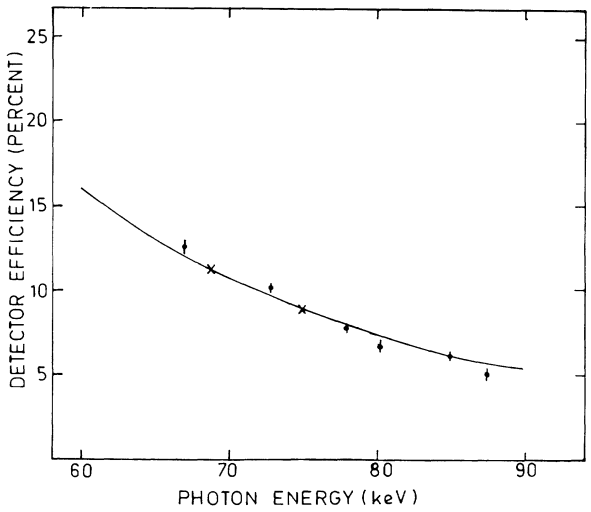

FIG. 2. Detector efficiency vs photon energy in the region of interest. The solid curve is based on the data supplied by the manufacturer. The data indicated by crosses are used for normalization. The data at other energies are obtained as discussed in Sec. II and shown along with the estimated errors. Only the ratios of efficiencies are needed in the determination of cross sections.

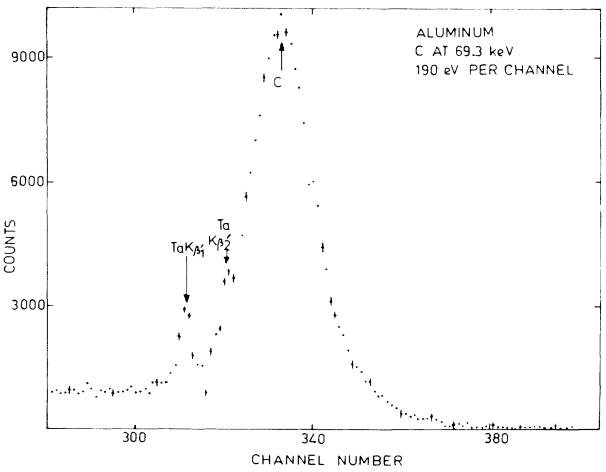

FIG. 3. Counts obtained with the help of an aluminum target in the neighborhood of the broad Compton peak vs channel number. The sharp peaks labeled as Ta $K\beta_1'$ and Ta $K\beta_2'$ are due to the characteristic x rays of the tantalum sleeve. C indicates the position of the Compton maximum.

and in lower channels the tails of the strong gold $K\beta_2'$ x-ray peak. The data obtained with bismuth reveal a broad peak in the neighborhood of 88 keV and a smaller but noticeable peak at about 89.9 keV. The higher-energy peak is observed only with a bismuth target and is clearly due to $K\beta_2'$ x rays of bismuth. The broadening on the lower-energy side of the 88-keV elastic scattering peak is due to $K\beta_1'$ x rays of bismuth. Note that the light elements in the bismuth compound target contribute negligibly, i.e., less than 0.5%, to the 88-keV elastic scattering intensity. The 88.03-keV γ rays cannot produce a vacancy in the K shell of bismuth. The appearance of the bismuth K x-ray peaks indicates that weak radiations of higher energy were present in the source. The data due to radiations directly from the source were measured in a separate experiment with a Si(Li) detector and also with a NaI(Tl) detector. Significant intensities of higher-energy γ rays were not found. Therefore, it was concluded that the undesirable higher-energy radiation must be primarily bremsstrahlung from a weak β contaminant in the source. This possibility has been confirmed by Amersham. Bismuth K x-ray intensities were typically about 2×10^{-3} of the K x-ray intensities measured with an equivalent lead target and indicate a source β component of a few percent. From the data presented in Ref. 4, it is apparent that such a contaminant was not present in the source used by the workers in Canada.

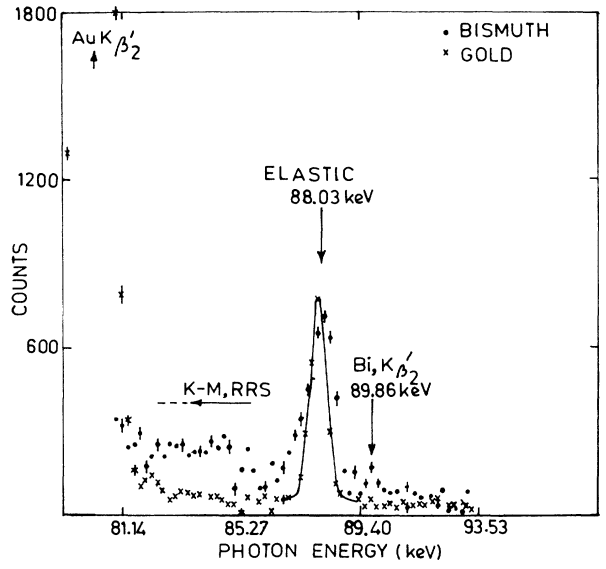

FIG. 4. Counts obtained with a gold target for energies above about 79.3 keV and with a bismuth target for energies above about 81 keV. The solid curve in the neigborhood of 88 keV is a fit to the elastic scattering counts determined with a gold target. The larger intensity between 81 and 85 keV obtained with the bismuth target in comparison with that obtained with the gold target is attributed to K-$M_{2,3}$ resonance Raman scattering. The small $K\beta_2'$ peak in bismuth data is caused by a weak higher-energy contaminant in the source (see Sec. II). The intense peak around 80 keV (not fully shown) is due to $K\beta_2'$ x rays of gold. Several such data sets were obtained.

The bismuth resonance Raman scattering (RRS) component is evident from the data in Fig. 4 below about 85 keV. For example, the K-M_3 RRS component is expected to appear at energies below $(88.03-B_{M_3})$ keV, where B_{M_3} is the binding energy of the M_3 subshell and is 3.177 keV in the case of bismuth. There is no characteristic x ray of bismuth with energy between 80 and 85 keV. In the same energy range, the bismuth data lie substantially above the corresponding gold data, although the bismuth counts in the neighborhood of 88 keV are somewhat less than the gold counts. Thus the higher bismuth counts between 80 and 85 keV cannot be due to a lower-energy tail of the peak around 88 keV. Of course, the K-M_2 RRS component is also expected to appear below 84.33 keV. A similar enhancement, not shown, was noticed in the bismuth data below 72.3 keV corresponding to the K-L_2 RRS component. The K-L_3 RRS component could not be seen clearly because it overlaps with the $K\alpha_2$ x rays of bismuth at 74.82 keV caused by the higher-energy source contamination mentioned in the previous paragraph. The observed bismuth RRS intensities are consistent with those reported in Ref. 4.

The data obtained with the bismuth target in the neighborhood of 69.3 keV were used to determine the Compton scattering cross section. For this purpose a relation similar to Eq. (1) was used. The ratio of the measured Compton scattering cross section to the Klein-Nishina prediction for a free electron gives the value of the incoherent scattering function $S(x,Z)$. On account of the strong intensity of $K\alpha$ x rays of gold and lead in the neighborhood of the expected Compton energy, values of $S(x,Z)$ could not be determined in these cases. However, another relation similar to Eq. (1) and $K\alpha_1$ x-ray counts instead of elastic scattering counts were used to estimate the K x-ray production cross sections in the case of gold and lead and therefrom the K-shell photoeffect cross sections. It should be noted that the detector efficiency ratios needed for these determinations have an error which is much smaller than the 5% error mentioned in the case of elastic scattering cross sections.

III. RESULTS AND DISCUSSION

Although definite evidence is obtained for resonance Raman scattering corresponding to K-L_2 and K-$M_{2,3}$ transitions in bismuth, cross sections for these processes are not reported for reasons outlined in Sec. II. The experimental values obtained for various other cross sections are summarized in Table I. In this table we also show our new S-matrix predictions obtained in independent-particle approximation in a Kohn-Sham potential with Latter tail, shifting the energy scale to coincide with experimental threshold energies. These represent the best currently available theoretical predictions.

We shall first discuss the elastic scattering cross sections. The first part of the discussion will show that the

TABLE I. Results obtained with 88.03-keV γ rays. The differential elastic scattering cross sections $d\sigma_{el}/d\Omega$ at 125° are given in column 2. Corresponding S-matrix predictions are given in column 3. The incoherent scattering function $S(x,Z)$ and K-shell photoeffect cross sections σ_K are listed in columns 4 and 5, respectively.

Element	$d\sigma_{el}/d\Omega$ (10^{-24} cm^2/sr) Experiment	Theory	$S(x,z)$	σ_K (10^{-24} cm^2)
Aluminum	0.0016±0.0002	0.00133		
Gold	0.711±0.049	0.680		1960±122
Lead	0.604±0.054	0.424		1760±114
Bismuth	0.221±0.020	0.132	68.6±4.7	

adopted experimental technique of normalization with respect to aluminum Compton counts is satisfactory. Referring to Eq. (1), one notices that only the elastic scattering counts n_{el}, the number N_{sc} of target atoms, and the effective target transmission factor T_{sc}^{88} are different in the case of different targets.

In the case of γ rays of energies as high as 88 keV incident on a low-Z target such as aluminum, the form-factor approximation is expected to give predictions accurate to about 1% for the Rayleigh amplitudes. We add the Rayleigh and the nuclear Thomson amplitudes and obtain a value of 1.32×10^{-27} cm^2/sr. The full S-matrix calculation is almost the same. The experimental value in Table I is slightly larger than this theoretical value. The deviation of (18±13)% between experiment and theory in this case should not cause serious concern in view of the difficulty of measuring a very small cross section with a weak source. Next we discuss the elastic scattering cross section of gold. Since the photon energy is only about 7.3 keV above the K-shell binding energy of gold, the form-factor approximation is expected to be unreliable for gold.

The experimental value of $(0.711\pm0.049)\times10^{-24}$ cm^2/sr agrees with the S-matrix prediction of 0.680. The calculation indicates a substantial suppression of the real amplitude from its form-factor value and a comparable magnitude imaginary amplitude. For lead, the photon energy is now only 25 eV above the K-shell threshold. The experimental value of $(0.604\pm0.054)\times10^{-24}$ cm^2/sr is significantly larger than the S-matrix prediction of 0.424. This prediction reflects a near-complete cancellation (at this angle) of the real amplitude and a cross section arising almost entirely from the imaginary amplitude. Here one may worry about the validity of independent-particle approximation (IPA), the determination of the threshold position, the effect of the large width of K-shell hole states,[12] etc. Some encouragement for the view that IPA is adequate for the imaginary amplitude follows from our observation (see below) of a photoeffect cross section within 10% of the IPA prediction. Finally, for bismuth the photon energy is now 2.5 keV *below* threshold. Experiment is substantially (70%) above theory, which again is due to a significant predicted cancellation of the real amplitude, but with a less important imaginary amplitude. The above-mentioned experimental results and IPA calculations suggest that the near-threshold departure of the real amplitude from the IPA prediction required for the explanation of experimental values is of the order of $1.5r_0$ in the case of lead and about $0.4r_0$ in the case of bismuth. Here the classical electron radius $r_0=e^2/4\pi\epsilon_0 mc^2$, e and m are the charge and mass of the electron, c is the velocity of light, and ϵ_0 is the permittivity of free space.

As a by-product, a value for the whole atom Compton scattering cross section was determined in the case of bismuth. The resulting value of the incoherent scattering function is (68.6±4.7), whereas the nonrelativistic tabulations[8] lead to a value of about 77 at $x=6.3$. A smaller deviation of the same sign between experimental and nonrelativistic values was noticed earlier in experiments[7] performed with 1.17- and 1.33-MeV γ rays at small scattering angles but for similar values of x.

The K-shell photoeffect cross sections measured in the case of gold and lead are, respectively, somewhat larger and smaller than the values 1770×10^{-24} cm^2 and 1968×10^{-24} cm^2 obtained by interpolation-extrapolation from the tabulations of Storm and Israel,[13] and of Scofield[14] for atomic cross sections. These values have errors of about 3%. The recent calculation of Tulkki[15] for radon gas atoms is useful for an understanding of departures from Scofield predictions when the photon energy is only slightly higher than the K-shell binding energy. In the present case, solid-state environment effects will also have to be considered.

The above discussions show that there is a significant deviation between experiment and existing theoretical calculations of elastic scattering near K-shell thresholds of high atomic number atoms. Further experimental and theoretical studies in this field will be very useful.

ACKNOWLEDGMENTS

The work was supported in part by Grant No. INT 82-13228 made by the National Science Foundation under the special Foreign Currency Program. The authors would like to thank Professor A. S. Mahajan and Professor V. L. Narasimham for reading the manuscript. One of the authors (K.M.V.) is grateful to University Grants Commission for additional support.

*Present address: Department of Physics, University of Warwick, Coventry CV4 7AL, United Kingdom.
†Permanent address: Department of Physics, University of Calicut, Calicut 673635, Kerala State, India.
‡Permanent address: Test Planning and Diagnostics Division, Sandia National Laboratories, Albuquerque, NM 87185.

[1]L. Kissel and R. H. Pratt, in *Atomic Inner Shell Physics,* edited by B. Crasemann (Plenum, New York, 1985), Chap. 10 and references mentioned therein.
[2]P. P. Kane, L. Kissel, R. H. Pratt, and S. C. Roy, Phys. Rep. **140**, 75 (1986).
[3]J. C. Parker and R. H. Pratt, Phys. Rev. A **29**, 152 (1984).
[4]J. K. MacKenzie and R. J. Stone, Solid State Commun. **55**, 751 (1985). This reference was kindly brought to our attention in a private communication from Dr. M. J. Cooper, University of Warwick, Coventry, England.
[5]B. Crasemann, M. H. Chen, and H. Mark, J. Opt. Soc. Am. B **1**, 224 (1984).
[6]S. Manninen, P. Suortti, M. J. Cooper, J. Chomilier, and G. Loupias, Phys. Rev. B **34**, 8351 (1986).
[7]P. P. Kane, J. Mahajani, G. Basavaraju, and A. K. Priyadarsini, Phys. Rev. A **28**, 1509 (1983).
[8]J. H. Hubbell, W. J. Veigele, E. A. Briggs, R. T. Brown, D. T. Cromer, and R. J. Howerton, J. Phys. Chem. Ref. Data **4**, 471 (1975); **6**, 615(E) (1975).
[9]J. L. Campbell, A. Perujo, W. J. Teesdale, and B. M. Millman, Phys. Rev. A **33**, 2410 (1986) and references mentioned therein.
[10]J. H. Scofield, Phys. Rev. A **9**, 1041 (1974).
[11]J. L. Campbell, P. L. McGhea, J. A. Maxwell, R. W. Ollerhead, and B. Whittaker, Phys. Rev. A **33**, 986 (1986).
[12]J. Bremer, J. Phys. B **12**, 2797 (1979).
[13]E. Storm and H. I. Israel, Nucl. Data Tables A **7**, 565 (1970).
[14]J. H. Scofield, Lawrence Radiation Laboratory Report No. UCRL 51326, 1973 (unpublished).
[15]J. Tulkki, Phys. Rev. A **32**, 3153 (1985).